Universiteit
Leiden
The Netherlands

Interference effects with surface plasmons

Kuzmin, N.V.

Citation
Kuzmin, N. V. (2008, January 10). *Interference effects with surface plasmons*. *Casimir PhD Series*. LION, Quantum Optics Group, Faculty of Science, Leiden University. Retrieved from https://hdl.handle.net/1887/12551

Version:	Corrected Publisher's Version
License:	Licence agreement concerning inclusion of doctoral thesis in the Institutional Repository of the University of Leiden
Downloaded from:	https://hdl.handle.net/1887/12551

Note: To cite this publication please use the final published version (if applicable).

Chapter 2

Plasmon-assisted two-slit transmission: Young's experiment revisited[1]

We present an experimental and theoretical study of the optical transmission of a thin metal screen perforated by two subwavelength slits, separated by many optical wavelengths. The total intensity of the far-field double-slit pattern is shown to be reduced or enhanced as a function of the wavelength of the incident light beam. This modulation is attributed to an interference phenomenon at each of the slits, instead of at the detector. The interference arises as a consequence of the excitation of surface plasmons propagating from one slit to the other.

[1]) H.F. Schouten, N.V. Kuzmin, G. Dubois, T.D. Visser, G. Gbur, P.F.A. Alkemade, H. Blok, G.W.'t Hooft, D. Lenstra, and E.R. Eliel, *Plasmon-assisted two-slit transmission: Young's experiment revisited*, Phys. Rev. Lett. **94**, p. 053901 (2005)

2.1 Introduction

Recently, there has been a surge of interest in the phenomenon of light transmission through sub-wavelength apertures in metal plates. This followed the observation of enhanced transmission through a two-dimensional hole array by Ebbesen *et al.* [36], who found that the transmission of such an array could be much larger than predicted by conventional diffraction theory [37]. This discovery has rekindled the interest in a similar but simpler problem, viz. the transmission of a one-dimensional array of sub-wavelength *slits* in a metal film, i.e., of a metal grating [36, 38–51]. In many cases the enhanced transmission of hole or slit arrays has been explained in terms of the excitation of (coupled) surface plasmons on the metal film [38–40, 42], an explanation that has recently been challenged [51]. It has been shown that, for slit arrays, Fabry-Pérot-type waveguide resonances can also give rise to considerably enhanced transmission [40, 41, 44, 45, 47].

2.2 Idea

In this chapter we study an even more fundamental system than the metallic grating, namely a thin metal layer perforated by just *two* parallel sub-wavelength slits. In contrast to the systems that have recently attracted so much attention, our slits are separated by *many* optical wavelengths. Thus we study the light transmission of a setup that lies at the heart of wave physics, namely that of Thomas Young. We do, however, not focus on the well-known interference pattern named after him, but on the angle-integrated power transmission coefficient of the perforated screen, i.e. the transmission integrated over many interference orders. We show that this transmission coefficient is strongly modulated as a function of the wavelength of the incident light for the case that that light is TM-polarized, i.e., with the electric field aligned perpendicular to the slits. In contrast, there is no such modulation when the incident light is TE-polarized, or when the "wrong" metal is chosen. All our observations can be explained in terms of a model involving the coherent transport of electromagnetic energy between the slits by surface plasmons.

2.3 Experiment

Our samples consist of a 200 nm thick gold film, evaporated on top of a 0.5 mm thick fused-quartz substrate with a 10 nm thick titanium adhesion layer between the gold and the glass. In such a sample a two-slit pattern is

written using a focussed ion beam [52], each slit being 50 μm long and 0.2 μm wide. The centers of the slits are separated by a distance, as measured with a scanning electron microscope, of 4.9, 9.9, 14.8, 19.8 or 24.5 μm, respectively. Such a two-slit pattern, with the metallized side facing the laser, is illuminated at normal incidence with the well-collimated output beam ($\approx$ 2 mm diameter) of a narrow-band CW Ti:sapphire laser, tunable between 740 and 830 nm. We detect in transmission, integrating the double-slit pattern over a large number of interference orders. The zeroth order peak is considerably stronger than the other orders, presumably as a result of non-negligible leakage through the bulk metal, and is therefore fully blocked by an opaque screen. We choose the polarization of the incident light to be either parallel (TE) or perpendicular (TM) to the long axis of the pair of slits.

2.4 Results

The results for the case of TM-polarization are shown in Fig. 2.1. The transmission is seen to be approximately sinusoidally modulated as a function of wave number, the modulation period being inversely proportional to the the slit separation. The visibility of the fringes is of order 0.2, roughly independent of the slit separation. Note that the fringes are superposed on an offset that gradually decreases as a function of wavelength.

When, instead, a TE-polarized beam is used to illuminate the double slit (24.5 μm slit distance) the detected signal shows no modulation whatsoever (see bottom frame of Fig. 2.1). Equally, no modulation is observed when the experiment is performed using a 200 nm thick titanium layer instead of gold, independent of the polarization of the incident radiation.

The observed strong polarization anisotropy and the dependence on the material of the screen both suggest that surface plasmons propagating along the gold/air interface lie at the heart of the observed phenomena. Alternative explanations in terms of waveguide modes within the slit [40, 41, 44, 45, 47] or diffractive evanescent waves [51] are excluded by the observed *dependence* of the spectral modulation period, and the *independence* of the modulation depth on the slit separation.

The surface plasmons cannot be excited on a smooth interface by the normally incident beam, because of translational invariance. In the present case the slits brake the translational symmetry of the surface and can provide the missing momentum along the interface. Thus, when the incident light is TM-polarized it excites, at each of the slits, a surface plasmon propagating along the interface between the metal and the dielectric. The propagation

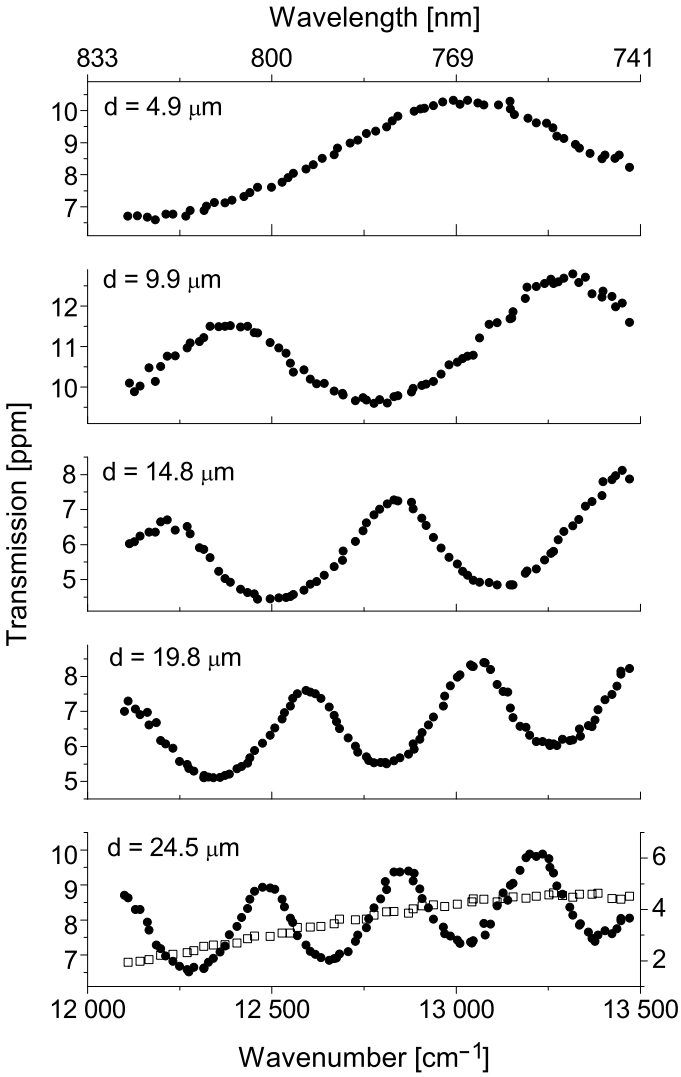

Figure 2.1. Experimental angle-integrated transmission spectra for a TM-polarized input beam (polarization perpendicular to the long axis of the 200 nm wide slits). The value of the slit separation d is indicated in each of the frames. In the frame at the bottom ($d = 24.5$ μm) the results for TE-polarized incident light (open squares) are included; the scale at the right applies to this choice of polarization.

Figure 2.2. Two interfering paths leading to light emission from the leftmost slit. A similar set of paths gives rise to emission from the slit on the right-hand side. The dashed line indicates the propagating surface plasmon.

constant k_{sp} of such a surface plasmon is given by [8]:

$$k_{\mathrm{sp}} = k_0 \sqrt{\frac{\epsilon_{\mathrm{m}}\epsilon_{\mathrm{d}}}{\epsilon_{\mathrm{m}} + \epsilon_{\mathrm{d}}}}, \tag{2.1}$$

where ϵ_{m} and ϵ_{d} are the complex (relative) dielectric constants of the metal and dielectric, respectively, and $k_0 = 2\pi/\lambda$ the free-space wave number. The surface-plasmon wavelength is related to the real part of k_{sp} by $\lambda_{\mathrm{sp}} = 2\pi/\mathrm{Re}(k_{\mathrm{sp}}) \equiv \lambda_0/n_{\mathrm{sp}}$, while its (amplitude) decay length is given by $1/\mathrm{Im}(k_{\mathrm{sp}})$. For the gold/air interface at $\lambda_0 = 800$ nm $n_{\mathrm{sp}} = 1.02$ and $1/\mathrm{Im}(k_{\mathrm{sp}}) \approx 80$ μm [53], considerably larger than the separation of the slits. Consequently, surface plasmons propagating along this interface can easily cover the distance between the slits. In contrast, the amplitude decay length for the Ti/air interface at $\lambda_0 = 800$ nm is only ≈ 7 μm [54], considerably shorter than the separation of most of our double slits. Surface plasmons launched on this interface simply do not survive long enough, as is confirmed by our experiments.

Since the gold film is sandwiched between glass ($\epsilon_{\mathrm{d}} \approx 2.1$) and air ($\epsilon_{\mathrm{d}} = 1$), the surface plasmons living on the Au/air and Au/glass interfaces have different (complex) propagation constants (see Eq. (2.1)). Moreover, a 10 nm film of Ti lies between the glass substrate and the gold film, resulting in a much reduced decay length of the surface plasmons on that interface. Consequently, of all the interfaces that we probe in the experiment, only the Au/air variety supports surface plasmons propagating over distances comparable to the separation of the slits.

A surface plasmon on this interface, excited at one of the two slits and traveling towards its partner slit, can scatter there, being converted to free-space radiation. Each propagating surface plasmon therefore generates an additional path for light transmission through the slit (see Fig. 2.2). The plasmon-mediated amplitude at the second slit interferes with the amplitude of the light that is directly transmitted by that slit. Consequently, the field amplitude at the second slit's dark side can be written as

$$E^{(2)}_{\mathrm{slit}} = E_0(\lambda_0)(1 + \alpha(k_{\mathrm{sp}}) \exp[i(k_{\mathrm{sp}} d + \Phi)]), \tag{2.2}$$

where d is the slit separation, $\alpha(k_{\mathrm{sp}})$ the relative strength of the plasmon contribution and Φ a phase factor, assumed to be wavelength-independent. The field amplitude $E^{(2)}_{\mathrm{slit}}$ behind the second slit is thus enhanced or suppressed, depending on the argument of the complex phase factor in Eq. (2.2). Because our laser beam is normally incident on the sample and symmetrically illuminates the two slits, the field amplitude behind the first slit is given by $E^{(1)}_{\mathrm{slit}} = E^{(2)}_{\mathrm{slit}}$.

In the present experiment the far-field two-slit pattern arises as a consequence of the interference of *four* paths, two of which are partially plasmonic, while the other two are photonic all the way. Although the number of interfering channels is four in the present experiment, the far-field pattern that arises behind the sample is simply that of Young's experiment, i.e. a pattern of *two* interfering sources. The novel aspect is that the strength of each of these sources is enhanced or reduced due to the interference of a photonic and a plasmonic channel.

We collect a large number of interference orders on our detector thereby effectively erasing the far-field two-slit pattern. Hence, the signal S picked up by our detector is simply proportional to the total power radiated into the acceptance angle of the detector, i.e., to twice the power radiated by each slit separately,

$$S \propto 2E_0^2(\lambda_0) \left[1 + \alpha^2(k_{\mathrm{sp}}) + 2\alpha(k_{\mathrm{sp}}) \cos(k_{\mathrm{sp}} d + \Phi)\right]. \tag{2.3}$$

From the experiment we estimate that, across the wavelength range probed, the parameter $\alpha(k_{\mathrm{sp}}) \approx 0.1$ and is independent of the wavelength of the incident radiation. Further, in order to reliably fit our experimental transmission spectra with the expression given by Eq. (2.3) and the measured values for the slit separation we need to take the dispersion of the surface plasmon's propagation constant into account. This provides additional support for our claim that the effect observed here is to be attributed to communication between the slits by propagating surface plasmons.

Surface plasmons can also be excited when the incident light is TE-polarized, in this case at the sub-μm top and bottom edges of the 50 μm long slits. These surface excitations do not effectively couple to the other slit, being predominantly emitted in the wrong direction. In the absence of plasmon-mediated inter-slit coupling the angular-integrated double-slit spectrum is expected to be smooth, and this is in line with our experimental findings (see Fig. 2.1).

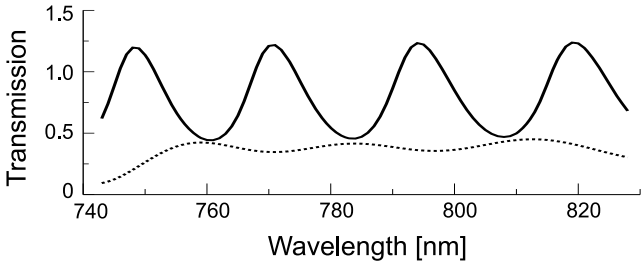

Figure 2.3. The calculated transmission coefficient T of a double slit in a 200 nm thick gold film as a function of the wavelength of the incident light. The slits are 200 nm wide and separated by 25.0 μm. The full line displays the results for TM polarization, while the dotted line (magnified 10 times) shows the results for the case of TE polarization. The transmission coefficient is normalized to the area of the slits.

Note that for this polarization the incident light is beyond cut-off for each slit separately.

2.5 Theoretical calculation

Theoretically, we calculate the transmission of the double-slit system using a rigorous scattering model based on a Green's function approach. We write the total electric field, $\mathbf{E}$, as the sum of the incident field, $\mathbf{E}^{(\mathrm{inc})}$, taken to be monochromatic and propagating perpendicular to the plate, and the scattered field, $\mathbf{E}^{(\mathrm{sca})}$. The former is the solution of the scattering problem (including multiple reflections) in the absence of the slits, while the latter is the field due to their presence. The total electric field can be written as [55, 56]

$$\mathbf{E} = \mathbf{E}^{(\mathrm{inc})} - \mathrm{i}\omega\Delta\epsilon \int_{\mathrm{slits}} \mathsf{G} \cdot \mathbf{E}\, \mathrm{d}^2 r, \tag{2.4}$$

where $\Delta\epsilon = \epsilon_0 - \epsilon_{\mathrm{m}}$ is the difference in permittivity of the slits (vacuum) and the metal plate, and G is the electric Green's tensor pertaining to the plate without the slits. We have suppressed the time-dependent part of the field given by $\exp(-\mathrm{i}\omega t)$, where ω denotes the angular frequency. Note that, for simplicity, we here assume that the metal film is embedded in air on both sides. For points within the slit Eq. (2.3) is a Fredholm equation of the second kind for $\mathbf{E}$, which is solved numerically by the collocation method with piecewise-constant basis functions [57]. To quantify the transmission process, a normalized transmission coefficient is used, where the geometrical optical transmission through the two slits is taken as the normalization factor [56].

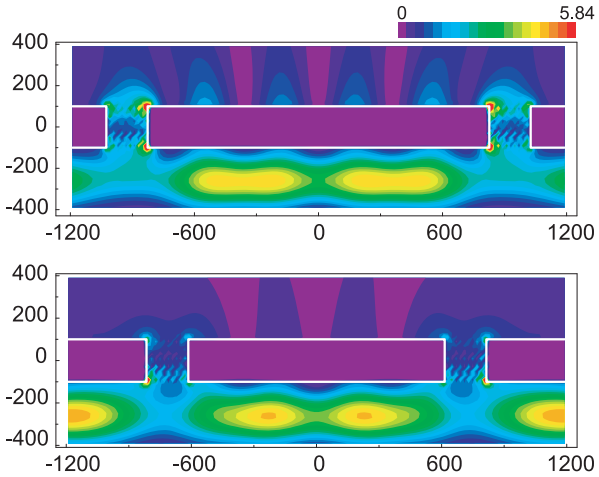

Figure 2.4. Intensity distribution in the immediate vicinity of the double-slit system for TM-polarized incident radiation when the transmission is maximum (top frame, slit separation equal to $5\lambda_{sp}/2$), and minimum (bottom frame, slit separation equal to $4\lambda_{sp}/2$)). The field is incident from below. All lengths are in nm.

The wavelength dependence of the dielectric constant of the gold film is fully taken into account [53].

In Fig. 2.3 the total transmission of the two-slit configuration is shown as a function of the wavelength of the incident radiation. When the incident field is TE polarized, the transmission of the double slit is small and weakly modulated as a function of wavelength. In contrast, for a TM-polarized incident field, the transmission shows a strong modulation as a function of wavelength with a visibility $\mathcal{V} \approx 0.45$. Overall the agreement between the experiment and the results of the Green's function model is seen to be good, the theoretical data having a somewhat larger visibility than the experimental ones ($\mathcal{V} \approx 0.2$). This difference can be attributed to the different embedding of the gold film in the experiment and in the calculation. While in the experiment the gold film is asymmetrically encapsulated, in the calculation the materials at either side of the film are identical, greatly enhancing the plasmonic effects.

Using the theoretical model outlined above we have also calculated the intensity distribution, i.e. the value of $|E|^2$, on both sides of a free-standing perforated gold film (see Fig. 2.4). For calculational convenience we have taken values of the slit separation that are considerably smaller than those of the experiment, viz. $5\lambda_{sp}/2$, where the transmission is maximum, and $4\lambda_{sp}/2$, where the transmission is minimum. In the first case (maximum transmission)

one can distinguish at the dark side of the metal film a well-developed standing wave pattern along the interface, having six antinodes, two of which coincide with the slits themselves. In contrast, when the transmission is minimum the antinodes of the standing-wave pattern do not coincide with the slits; at these locations one rather finds a node of the standing-wave pattern. In both cases the intensity is seen to rapidly decay away from the air-metal interface.

2.6 Conclusions

In this Chapter we have shown that Young's double slit experiment, often seen as proof of the wave nature of light, can provide powerful evidence for the role of propagating surface plasmons in the transmission of perforated metal screens. The transport of electromagnetic energy by the surface plasmons over distances of many optical wavelengths gives rise to an interference phenomenon in the slits that enhances or reduces the intensity of the far-field pattern.

2.7 Appendix: Erasing the interference (unpublished)

In Chapter 2 we studied the transmission spectrum of a metallic film containing two close-lying sub-wavelength wide slits at normal incidence. The observed spectral modulation is explained in terms of plasmonic cross-talk, i.e., a coherent energy transport from one slit to the other by means of surface plasmons. Due to this process a fraction of the light incident on slit A emerges from slit B where it interferes with a fraction of the light incident on that same slit. This interference effect takes place in both slits and at normal incidence the relative phases of the two interfering channels in the two slits $\Delta\phi_{\mathrm{A}}$ and $\Delta\phi_{\mathrm{B}}$ are equal.

Here we study the transmission spectrum of such a double slit at non-normal incidence.

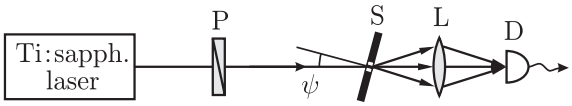

Figure 2.5. Experimental setup for measuring the transmission spectrum of a double slit.

The experimental arrangement is shown in Fig. 2.5. The TM-polarized collimated output beam from a wavelength-tunable Ti-sapphire laser ($743 < \lambda < 827$ nm) is incident on our sample at near-normal incidence, with a beam diameter of $\approx$ 2 mm. The transmitted light is collected and imaged on a Si-photodetector. We scan the wavelength of the laser and measure the photodetector signal. The latter is normalized by means of the signal from a second photodetector that monitors the laser output power. Our sample consists of a 200 nm thick gold film on top of a 0.5 mm thick glass substrate with a 10 nm thick titanium adhesion layer in between. Two 50 μm long, 0.2 μm wide, parallel slits with a separation of $d = 24.5$ μm, have been ion-beam-milled in the gold film. We record the normalized transmission spectrum of this double-slit system for various angles of incidence. The experimental results are shown in Fig. 2.6a, for angles of incidence of $0°, 0.5°, 1°, 3°$ and $5°$ (from top to bottom). A couple of features are noteworthy. First, when comparing the spectra at $0°$ and $1°$ angles of incidence one notices that they seem to have flipped: where one spectrum shows a maximum, the other shows a minimum, and vice versa. Second, some of the spectra appear to be featureless in certain spectral regions, for instance the spectrum at $3°$ angle of incidence for $743 < \lambda < 762$ nm.

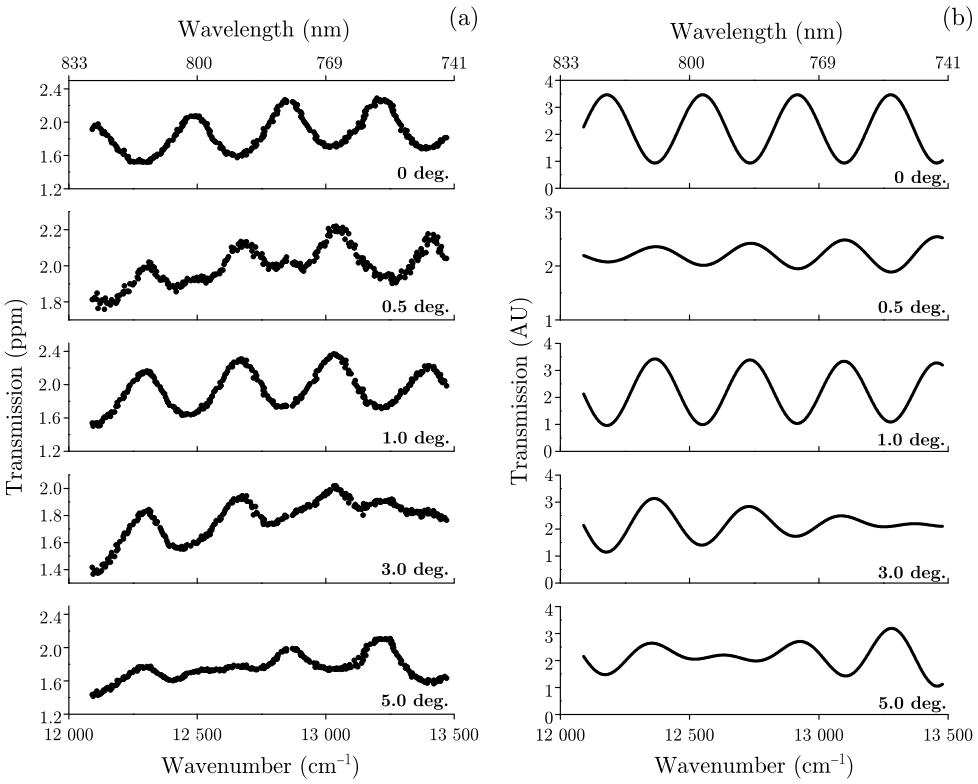

Figure 2.6. Experimental (a) and calculated (b) two-slit transmission spectra for angles of incidence of $0°, 0.5°, 1°, 3°$ and $5°$ (from top to bottom).

These observations can be explained by realizing that, at non-normal incidence, the relative phases $\Delta\phi_{\mathrm{A}}$ and $\Delta\phi_{\mathrm{B}}$ of the interfering channels in slits A and B are no longer equal (see Fig. 2.7). The fields in the two slits can be written as:

$$E_{\mathrm{A}} = E_0[1 + \alpha \exp\{i(k_{\mathrm{sp}}d + \Phi)\} \exp\{i\Delta\phi\}], \quad (2.5)$$

$$E_{\mathrm{B}} = E_0[\exp\{i\Delta\phi\} + \alpha \exp\{i(k_{\mathrm{sp}}d + \Phi)\}], \quad (2.6)$$

where α is the surface-plasmon coupling coefficient and Φ a coupling phase, both of which are introduced in Chapter 2, and $\Delta\phi = k_0 d \sin\psi$ is the extra phase accrued by the light when traveling to slit B, with k_0 the wave vector of free space.

The detector signal $S(\lambda)$ can now be calculated[1] by evaluating $|E_A|^2 + |E_B|^2$,

$$S(\lambda) = S_0[1 + \alpha^2 + 2\alpha\cos(k_{sp}d + \Phi)\cos(k_0 d\sin\psi)]. \tag{2.7}$$

It is seen that the term $2\alpha\cos(k_{sp}d + \Phi)$, describing the spectral modulation, is itself amplitude modulated by the term $\cos(k_0 d\sin\psi)$. Whenever the latter term goes to zero, the plasmon-induced spectral modulation is suppressed. Figure 2.6b shows the spectra according to Eq. (2.7) for $\alpha = 0.2$ and $\Phi = \pi$ (see Chapter 5).

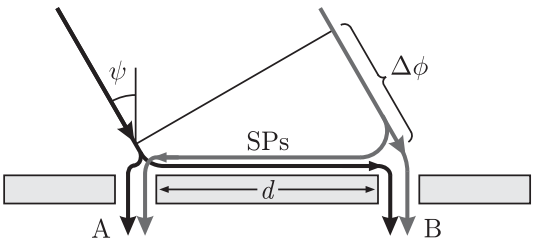

Figure 2.7. Pathways of light and surface plasmons when the sample is illuminated at an angle of incidence equal to ψ.

We find good agreement between the calculated and observed modulation spectra. Note that the spectral modulation at an angle of incidence of 0.5° is calculated to be almost erased. This can be understood by evaluating the quantity $k_0 d\sin\psi$, which varies between 0.52π and 0.58π across the wavelength range studied so that $\cos(k_0 d\sin\psi) \approx 0$. The observed phase shift of the modulation pattern upon changing the angle of incidence from 0° to 1° is due to the fact that $k_0 d\sin\psi$ goes from 0 to $\approx \pi$.

Another way to look at the erasure phenomenon is by realizing that the spectral modulation originates in an interference phenomenon in each of the slits. The modulation being erased implies that, at the detector, the interference is made to vanish. By writing the signals from slits A and B as:

$$S_A = S_0[1 + \alpha^2 + 2\alpha\cos(k_{sp}d + \Phi + \Delta\phi)], \tag{2.8}$$
$$S_B = S_0[1 + \alpha^2 + 2\alpha\cos(k_{sp}d + \Phi - \Delta\phi)], \tag{2.9}$$

we realize that the spectral modulation in S_A is π out of phase with that in S_B whenever $\Delta\phi = \pi/2 + m\pi$, with m an integer.

[1] A bucket detector is used to collect most of the interference orders such that the spatial information is effectively erased.

Clearly, the plasmon-induced modulation of the two-slit transmission spectrum is quite sensitive to the angle of incidence of the illuminating light. That implies that one has to be quite careful when illuminating the sample with a focussed beam, as such a beam can be described as a superposition of plane waves at different angles of incidence. With a strongly focussed beam it is quite possible to wash away most of the modulation features in the transmission spectrum of the double slit.